Electromagnetic design and analysis of a PM motor with HTS bulk

Huo H. K., Qiu M., Xia D., Xu Z., Lin L.Z.

Institute of Electrical Engineering, Chinese Academy of Sciences, Beijing 100080, P.R. China

Melt-processed HTS bulk with approximately single-domain structure can trap a magnetic field exceeding 2 T at 77 K. So the flux-trapped superconductor is regarded as a magnet superior to conventional permanent magnet, which can be used for electrical motor. A PM electrical motor with HTS bulk was designed in theory and analyzed by FEA. The magnetization method for HTS bulk in the motor was discussed in detail and simulated using the flux flow-creep model. The experiment was also carried out to test the validity of the simulation.

INTRODUCTION

Melt-Processed YBCO bulk superconductor with approximately single domain structure can trap a magnetic field exceeding 2 T at 77 K [1]. Hence, the flux-trapped superconductor has been regarded as a magnet superior to conventional permanent magnet such as Nd-Fe-B. We designed a theoretic model of permanent synchronous electrical motor, in which conventional permanent magnets are replaced by YBCO HTS bulks and simulated it with ANSOFT. The magnetization method for HTS bulk in the motor was discussed, and simulated by flux flow-creep model.

STRUCTURE DESIGN OF THE HTS MOTOR

The stator of the HTS PM motor is the same as that of the conventional synchronous motor. The stator coils are wound from a bundle of 528 Cu wires, each 0.8 mm in diameter and electrically insulated. As we know, conventional 3 phases winding in the slots of the stator can produce rotating field, if there are symmetrical 3 phases electrical current flowing in them. The rotor of the motor is made up of laminated irons, axle, squirrel cage, magnetizing coil and YBCO bulks serving as the permanent magnet. The rotor and the stator are immersed in liquid nitrogen. Before staring the motor, the YBCO bulk is magnetized first by the magnetizing coil. The rated capacity and rated voltage of the motor in theory are 0.8 kW and 220 V, respectively. Inner diameter and outer diameter of the stator are 162 mm and 245 mm, respectively. Table 1 shows the parameters of the HTS synchronous motor that we designed in theory.

Table 1   Parameters of the HTS PM synchronous motor designed in theory

Rated power P_N=800 W	Rated voltage U_N=220 V	Rotating speed n_N=1000 r/min
Frequency f=50 Hz	Inner diameter D_1=0.162 m	Outer diameter D_2=0.245 m
Pole distance τ=0.0848 m	No of phase m=3	Height of bulks h=8 mm
Length of axis c=58 mm	Width of bulks a=35 mm	Width of air gap g=0.8mm
Bundle of Cu wires in stator W=528	Diameter of Cu coil D_3=0.8 mm	Number of the stator slots Z_1=36
Number of the rotor slots Z_2=46	Connection mode Y	Trapped field of bulks B=1 T

The rotor speed is synchronous to the rotating stator speed, which is 1000 rpm at 50 Hz for a 6-pole motor. The interaction between rotating field and rotor field results in a force along the surface and produce the output torque.

PULSE FIELD MAGNETIZATION

The YBCO bulks used in this motor are magnetized by the magnetizing coil with pulsed current, which is produced by voltage source through discharging a series of capacitors. Remnant Magnetic fields are measured by three Hall sensors placed at the center, periphery, and the midpoint on the top surface of the bulk at 77 K. We use flux flow-creep model to simulate the magnetization process, and compare the results with our experiments.

The governing equations for both superconductors and normal conductors are derived form Maxwell's equations. In cylindrical coordinates, the axisymmetric scalar equation is written as

$$\left(\frac{1}{r} \frac{\partial}{\partial r} \left(r \frac{\partial}{\partial r} \right) + \frac{\partial^2}{\partial z^2} - \frac{1}{r^2} \right) A = -\mu_0 J \tag{1a}$$

$$E = -\frac{\partial A}{\partial t} \tag{1b}$$

where μ_0 is the magnetic permeability in vacuum, E is the electric field, B is the magnetic flux density, and A is the magnetic vector potential. Nonlinear relationship between shielding current density and electric field is described by the flux flow-creep model and power law model.

$$E = 2\rho_c J_c \sinh\left(\frac{U_0}{kT} \frac{J}{J_c} \right) \exp\left(-\frac{U_0}{kT} \right) \quad \text{for flux creep region} \tag{2a}$$

$$E = \rho_c J_c + \rho_f J_c \left(\frac{J}{J_c} - 1 \right) \quad \text{for flux flow region} \tag{2b}$$

where ρ_c is the creep resistivity, ρ_f is the flow resistivity, U_0 is the pinning potential, T is the temperature, and k is the Boltzman constant. The nonlinear dependence of critical shielding current on magnetic field is considered by using the Kim model and on the temperature is described also. The temperature distribution in the bulk is obtained through solving the heat diffusion equation:

$$J_C(|B|) = \frac{J_{C0} B_0}{(|B| + B_0)} \tag{3}$$

$$J_{C0}(T) = \alpha \left\{ 1 - \left(\frac{T}{T_{C0}} \right)^2 \right\}^2 \tag{4}$$

$$m_0 C \frac{dT}{dt} = \kappa_{ab} \frac{\partial^2 T}{\partial r^2} + \kappa_{ab} \frac{1}{r} \frac{\partial T}{\partial r} + \kappa_c \frac{\partial^2 T}{\partial z^2} + Q \tag{5}$$

where $m_0, C, \kappa_{ab}, \kappa_c$ are the density, specific heat, heat conductivities along the a-, b-axes, and heat conductivities along the c-axes, respectively. An iterative method is applied for the calculation of the shielding current and the magnetic field, ie.,

1. The artificial electrical conductivity σ is set to a special value.
2. The shielding current density is obtained by equations (1a), (1b)
3. The electric field is obtained by solving equations (2a), (2b), (3), (4) and (5)
4. The conductivity is modified by equations (1a) and (1b).
5. Steps 2-4 are repeated until σ is converged.

Table 2 shows parameters in the present numerical analysis.

Table 2　Parameters used in numerical simulation

$J_c = 10^7\ A/m^2$	$U_0 = 0.1 eV$	$\rho_f = 7.0 \times 10^{-10}\ \Omega m$	$C = 1.32 \times 10^2\ J/kg \cdot K$
$m_0 = 6.31 \times 10^3\ kg/m^3$	$\kappa_{ab} = 14.5 W/m \cdot K$	$\kappa_c = 3.0 W/m \cdot K$	$B_0 = 0.4$

The pulsed current plotted in Figure 1 is produced by voltage source through discharging a series of capacitors, which has been charged in advance. The maximum of the magnetic field in the coil during the pulsed field magnetization is 1 T. Magnetic fields are measured by Hall sensors placed at center, periphery, and the midpoint on the top surface of the bulk at 77 K. Figure 2-4 show the experimental results which are recorded, and used to compare with the simulation results.
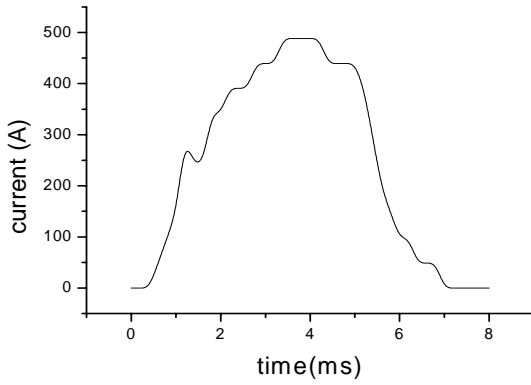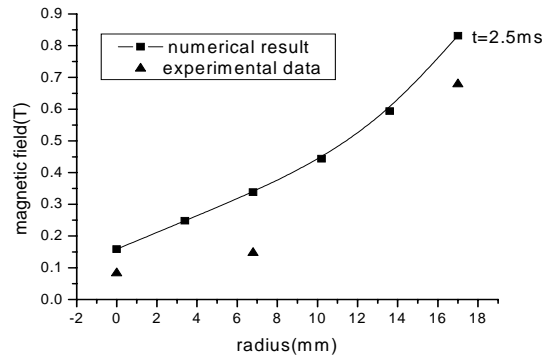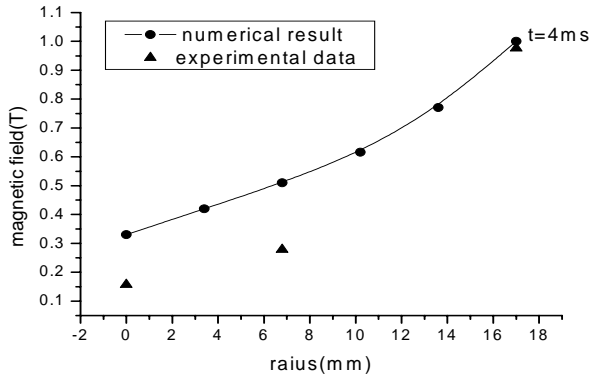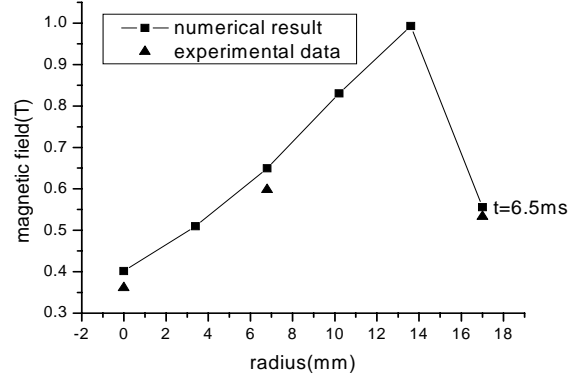

Figure 1　Pulse current flowing in the coil

Figure 2　Magnetic field when t=2.5 ms

Figure 3　Magnetic field when t=4.0 ms

Figure 4　Magnetic field when t=6.5 ms

When the pulsed field is applied to the bulk, the field changes from zero to a small value and the shielding current comes forth, which prevents the magnetic field from penetrating into the bulk. So the magnetic flux cannot enter the center of bulk at the beginning. With the increase of pulsed field, the magnetic field begins to penetrate into the center of the bulk step by step. We can see in Figure 4 that the magnetic field penetrates into the center of the bulk when time is 2.5 ms. On the decrease of the pulse field, shielding current is produced from outside of the bulk. The inner field of the bulk is still increasing after the peak of the external field, which was caused by the flux flow. From these figures we can see that the FFC model is better than the power law model in describing the PFM.
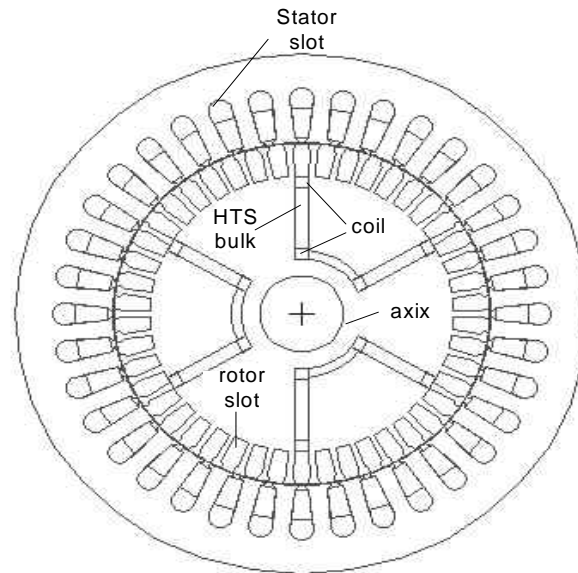
SIMULATION RESULTS OF THE MOTOR

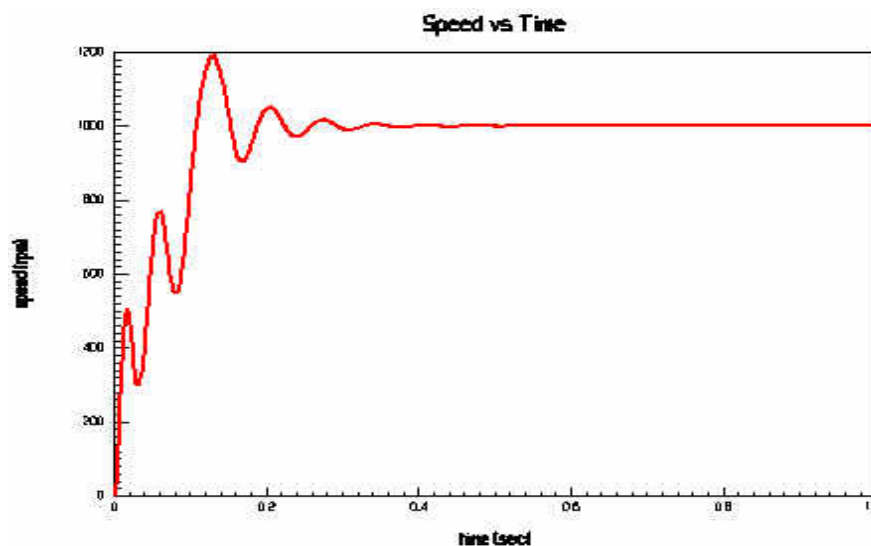Figure 5   Cross section of the HTS PM motor

Figure 6   Speed curve of the HTS PM motor with time

Figure 5 shows the cross section of the HTS asynchronous motor. In Figure 6, the speed serving as a function of the time is nearly constant and equal to the synchronous speed after 0.5 s. It can be seen that this HTS PM synchronous motor will be stable after 0.7s.

ACKNOWLEDGMENT

REFERENCE

[1] Itoh Y., and Mizutani U., Pulsed Field Magnetization of Melt-processed Y-Ba-Cu-O Superconducting Bulk Magnets, Jpn. J. Appl. Phys. (1996) 35 2114-2125.

[2] Tsuchimoto M., Morikawa K., Macroscopic Numerical Evaluation of Heat Generation in a Bulk High Tc Superconductor during Pulsed Field Magnetization, IEEE Trans. Appl. Superconductivity (1999) 9 66-70.